


Article

Flexural Performance of a New Hybrid Basalt-Polypropylene Fiber-Reinforced Concrete Oriented to Concrete Pipelines

Zhiyun Deng ^{1,2,*}, Xinrong Liu ^{2,*}, Ninghui Liang ², Albert de la Fuente ^{3,*}  and Haoyang Peng ¹

¹ Department of Hydraulic Engineering, Tsinghua University, Beijing 100084, China; phy17@mails.tsinghua.edu.cn

² School of Civil Engineering, Chongqing University, Chongqing 400045, China; lnh83249@cqu.edu.cn

³ Department of Civil and Environmental Engineering, Universitat Politècnica de Catalunya (UPC), Jordi Girona 1-3, 08034 Barcelona, Spain

* Correspondence: dzhy@mail.tsinghua.edu.cn (Z.D.); liuxrong@cqu.edu.cn (X.L.); albert.de.la.fuente@upc.edu (A.d.l.F.)

Abstract: The bending performance of a basalt-polypropylene fiber-reinforced concrete (HBPFRFRC) was characterized by testing $24,400 \times 100 \times 100$ mm³ prismatic specimens in a four-point bending test JSCE-SF4 configuration. The type and content of both fibers were varied in order to guarantee different target levels of post-cracking flexural performance. The results evidenced that mono-micro basalt fiber reinforced concrete (BFRC) allows the increase of the flexural strength (pre-cracking stage), while macro polypropylene fiber reinforced concrete (PPFRC) can effectively improve both bearing capacity and ductility of the composite for a wide crack width range. Compared with the plain concrete specimens, flexural toughness and equivalent flexural strength of macro PPFRC and the hybrid fiber-reinforced concrete (HFRC) increased by 3.7–7.1 times and 10–42.5%, respectively. From both technical and economic points of view, the optimal mass ratio of basalt fiber (BF) to polypropylene fiber (PPF) resulted in being 1:2, with a total content of 6 kg/m³. This HFRC is seen as a suitable material to be used in sewerage pipes where cracking control (crack formation and crack width control) is of paramount importance to guarantee the durability and functionality of the pipeline as well as the ductility of the system in case of local failures.

Keywords: basalt-polypropylene fiber-reinforced concrete; flexural performance; residual strength; optimal ratio



Citation: Deng, Z.; Liu, X.; Liang, N.; de la Fuente, A.; Peng, H. Flexural Performance of a New Hybrid Basalt-Polypropylene Fiber-Reinforced Concrete Oriented to Concrete Pipelines. *Fibers* **2021**, *9*, 43. <https://doi.org/10.3390/fib9070043>

Academic Editor:
Theodoros Rousakis

Received: 22 April 2021
Accepted: 1 June 2021
Published: 1 July 2021

Publisher's Note: MDPI stays neutral with regard to jurisdictional claims in published maps and institutional affiliations.



Copyright: © 2021 by the authors. Licensee MDPI, Basel, Switzerland. This article is an open access article distributed under the terms and conditions of the Creative Commons Attribution (CC BY) license (<https://creativecommons.org/licenses/by/4.0/>).

1. Introduction

It is well known that concrete is one of the most widely used civil materials for various engineering applications, such as hydraulic engineering, architectural engineering, road and bridge engineering. However, the concrete used in engineering usually had a large number of cracks, thus making the concrete brittle and subject to varying degrees of damage under external loads [1]. For the safety and reliability of concrete structures, higher requirements should be put forward for the energy dissipation capacity of concrete. FRC not only improves the brittleness of concrete but also significantly enhances the toughness and energy dissipation capacity of concrete [2–5]. Thus, FRC has become a widely used composite building material [6,7].

At present, many countries in the world have successively established the standard test methods for testing the bending performance of fiber reinforced concrete, such as JSCE-SF4 [8], ASTM C1018 [9] and CECS 13:2009 [10]. These standards provide a precise calculation method for the flexural strength, flexural toughness index and energy absorption of fiber reinforced concrete materials. Table 1 gathers relevant references related to the flexural characterization of FRCs with different types of fibers and amounts.

Table 1. Studies on the flexural performance of fiber reinforced concrete.

Type of Fibers	Φ_f/λ_f	Volume of Fibers (%)	f_c (MPa)	Height \times Width \times Length (mm ³)	Author
SF; MSF	SF: 50; MSF: 48–158	0.22–0.74	40.9–50.2	150 \times 150 \times 550	Buratti et al. [11]
SF	37.5–81.3	8	200	100 \times 100 \times 500	Nicolaides and Markou [12]
SF; PPF	SF: 83; MSF: /	SF: 0.51; PPF: 0.51	52.2	150 \times 150 \times 600	Pujadas et al. [13]
PPF	64.5	0.33, 0.49, 1.10	28–31	100 \times 100 \times 430	Enfedaque et al. [14]
SF; PPF	SF: 40, 60, 80; PPF: 280	SF: 0.5, 1.0, 1.5, 2.0; PPF: 0.1, 0.15, 0.2	47.5–58.1	100 \times 100 \times 400	Li et al. [15]
SF	37.5	1.78	82.1	100 \times 100 \times 350	Mínguez et al. [16]
SF; PVAf	SF: 56; PVAf: 308	SF: 0.5, 1.0, 1.5; PPF: 0.5, 1.0, 1.5	/	100 \times 100 \times 400	Liu et al. [17]
SF	65	0.26, 0.52, 0.77	21.3–28.1	150 \times 150 \times 600	Carrillo et al. [18]
SF	65	1, 2, 2.5, 7	152.1	40 \times 40 \times 160	Ferdosian and Camões [19]
SF; PPF	SF: 40; PPF: 200	SF: 2.0, 2.5, 3.0; PPF: 0.12, 0.17, 0.22	60.1–66.1	100 \times 100 \times 400	Guo et al. [20]
SF	80	0.075; 0.1	/	150 \times 150 \times 550	Meng et al. [21]

Note: SF means steel fiber; MSF means macro-synthetic fibers; PPF means polyolefin fiber; PVAf means polyvinyl alcohol fiber; f_c means compressive strength; / means lack of information; Φ_f/λ_f means aspect ratio.

Table 1 allows confirming that there exists extensive research on flexural performance of fiber reinforced concrete and that this topic is of interest from both scientific and industrial perspective. The general conclusion that can be extracted from the previous research is that the use of steel, polyolefin and/or polypropylene fibers, can largely improve the flexural performance of concrete. The mechanical properties of concrete reinforced with different types of hybrid fibers, which is termed hybrid FRC (HFRC), are usually superior to that of concrete reinforced with mono-fiber [22–25], HFRC is produced to achieve overall improvement both in energy absorption capacity and tensile strength. It is well known that coarse and long fibers control the propagation of macro-cracks and improve the toughness at the post-crack region [26,27], while micro and short fibers bridge the micro-cracks, thereby enhancing the peak strength [28]. So, the combination of different lengths, diameters and elastic modulus of fibers are often adopted by researchers [29–31]. An example of HFRC is the hybrid steel-polypropylene fibers (see Table 1), which are also used and confirmed to have obtained good hybrid effects [32–35]. However, steel fiber is easy to corrode, which is not conducive to the long-term stability of the structure. Moreover, the incorporation of steel fiber will not only reduce the workability of concrete but also increase the weight of concrete [36,37]. Therefore, under certain environmental conditions (such as an acidic environment), it is necessary to use corrosion-resistant material instead of steel fiber to improve the flexural performance of concrete.

A suitable material to substitute steel fiber is BF, which is characterized by good temperature stability, high tensile strength, strong corrosion-resistance, good deformation performance, low price, safe and environmental protection, etc. [38–40]. In addition, it has been confirmed that HBPFRC can show excellent crack propagation inhibition, fire resistance and flexural performance [41–45]. However, in the above studies, PPFs are all fine fibers, while the previous study [46] has shown that the improvement effect of macro PPFs on the bending properties of concrete is significantly superior to that of micro PPFs.

Therefore, micro BF and macro PPF are selected to be mixed into the concrete matrix to produce HBPFRC specimens. Furthermore, according to the Code CECS 13:2009 [10], the flexural performance of HBPFRC specimens was investigated by the four-point bending tests. This paper studies the flexural properties of HBPFRC, which indicates that this HFRC composite is a suitable material to be used in structures, such as sewerage pipes, where cracking control is of vital importance to guarantee the durability and functionality of the pipeline as well as the ductility of the system in case of local failures.

2. Materials and Methods

2.1. Test Material

The cement adopted in this test is Portland cement P.O.52.5. The coarse aggregate used were stones with grain sizes of 10–20 mm and 5–10 mm, while the fine aggregates were

sands of dimensions less than 5 mm. In addition, a commercially available polycarboxylic acid superplasticizer was adopted to improve concrete workability, and the water reducing rate of it is 28%. The concrete mix proportion is shown in Table 2.

Table 2. Concrete mix proportion.

Materials	Mass (kg/m ³)
Cement	375
Coarse aggregate 10~20 mm	545
Coarse aggregate 5~10 mm	545
Sand	850
Water	135
Water reducer	3.75

The fibers used in this test are macro PPF with a wavy surface and micro BF with a smooth surface, as shown in Figure 1 [47].

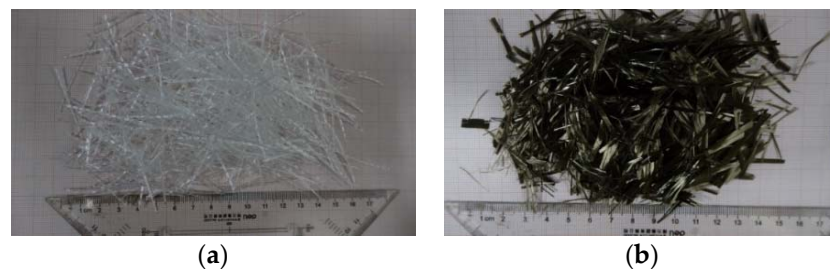


Figure 1. External shapes of fibers. (a) PPF; (b) BF [47]. (Reprint with permission [47]; 2021, Wiley).

In addition, the properties of the selected fibers are shown in Table 3.

Table 3. Properties of the selected fibers [47]. (Reprint with permission [47]; 2021, Wiley).

Fiber Type	BF	PPF
Diameter (mm)	0.013	0.8
Length (mm)	19	50
Tensile strength (MPa)	3300–4500	706
Aspect ratio	1460	63
Density (g/cm ³)	2.75	0.95
Elongation (%)	2.4–3.0	10
Elastic modulus (GPa)	95–115	7.4
Shape	straight	corrugated

2.2. Test Material Preparation

There are eight groups of HBPFRFC with different fiber content, including two groups of mono-fiber, five groups of hybrid basalt-polypropylene fiber as well as one control group (no fiber). Details of each group specimen for the flexural bending test are shown in Table 4.

Table 4. Details of each group specimen.

Specimen	The Fiber Content in kg/m ³ (% in Volume)	
	BF	PPF
B0.0P0.0	0.0 (0%)	0.0 (0%)
B0.0P6.0	0.0 (0%)	6.0 (0.63%)
B6.0P0.0	6.0 (0.22%)	0.0 (0%)
B1.2P4.8	1.2 (0.04%)	4.8 (0.51%)
B2P4	2.0 (0.07%)	4.0 (0.42%)
B3.0P3.0	3.0 (0.11%)	3.0 (0.32%)
B4.0P2.0	4.0 (0.15%)	2.0 (0.21%)
B4.8P1.2	4.8 (0.17%)	1.2 (0.13%)

As shown in Table 4, fiber contents ranged between 0 and 6 kg/m³. Amount of 4 kg/m³ of PPFs was considered the lower bound to provide ductility of the composite respect the unreinforced concrete [48,49] whilst 6 kg/m³ was fixed as an upper bound since higher amounts may compromise the workability and the finishing [50–54]. The select of ratio between fiber content of BF and PPF referred to the previous research results [47,53,54].

The mixability of fiber is very important to improve the performance of fiber reinforced concrete. In order to make the fibers evenly distributed into the concrete, referring to relevant specification and literature [10,47], the mixing process adopted in this experiment is as follows: (1) Pour the pre-weighted coarse and fine aggregates into the forced mixer and mix the materials for 1 min. (2) Evenly scatter the macro PPF and BF into the mixer, and the mixing process still lasted for 2 min after the fibers are all put into the mixer. (3) Pour the cement into the mixer and start mixing for 1 min. (4) Pour the water and water reducer slowly and evenly into the mixer and keep mixing for minutes. (5) Pour out the mixture and then pour them into the mold to produce HBPFR specimens. Part of the production and curing procedures of HBPFR specimens are shown in Figure 2.

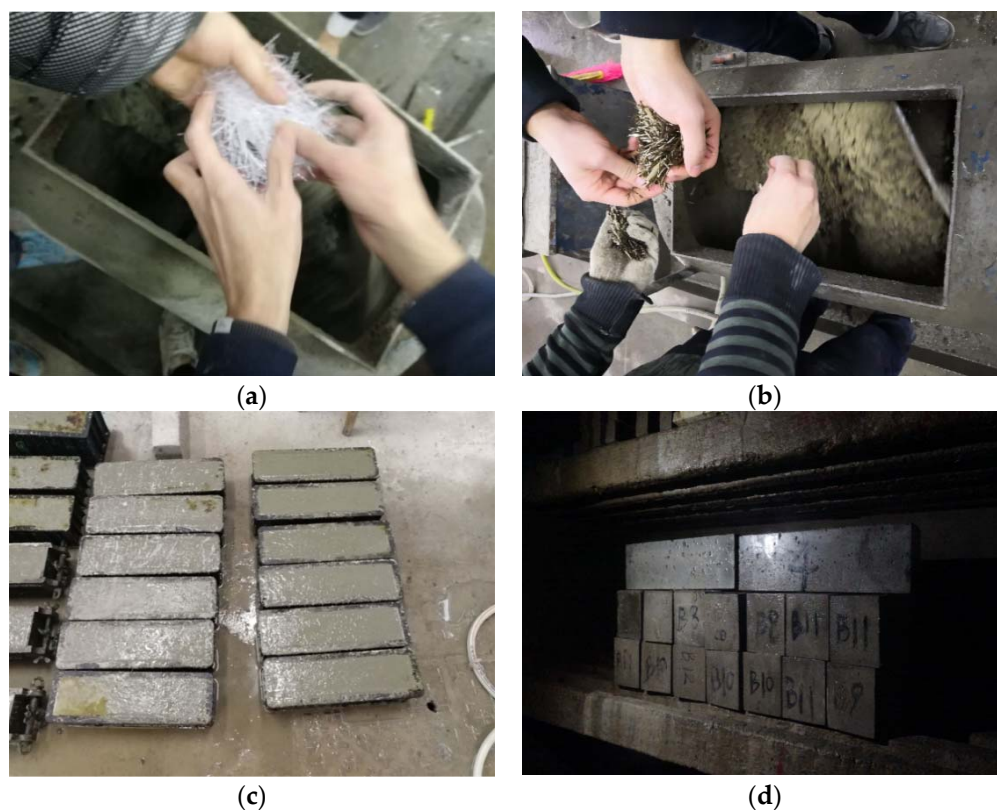


Figure 2. Partial production procedures of specimens. (a) Inclusion of PPF; (b) Inclusion of BF; (c) Specimen casting; (d) Specimen maintenance.

In this test, each group contained three replicate specimens. According to CECS 2009 [10], a total of 24 concrete specimens with a length \times width \times height of 400 mm \times 100 mm \times 100 mm were produced, and the four-point bending test was conducted after 28 days of curing.

2.3. Experimental Test Method

The four-point bending test was conducted to measure the flexural bending performance of concrete. The test device was the INSTRON–1346 hydraulic servo testing machine system. YOKE method is used to measure the deflection of beams [8]. Displacement control was adopted for continuous loading in the test, and the loading rate was 0.1 mm/min. After the deflection of the specimen reached 4 mm, the test was stopped. The test process was shown in Figure 3.

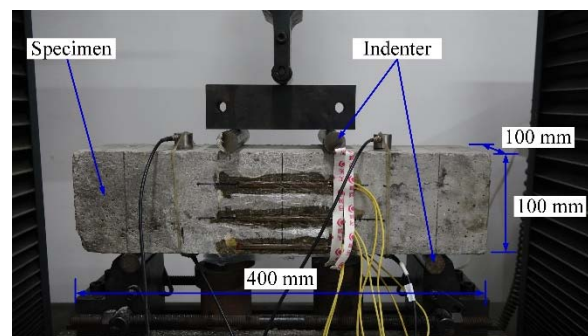


Figure 3. Test process diagram.

3. Test Results

3.1. Failure Modes

As the failure modes of each group of HBPFR specimens are similar, the failure modes of B2P4 are selected to represent that of the other HBPFR specimens. The failure modes of the control group specimen, the mono FRC specimen and the HBPFR specimen are shown in Figure 4a–d.

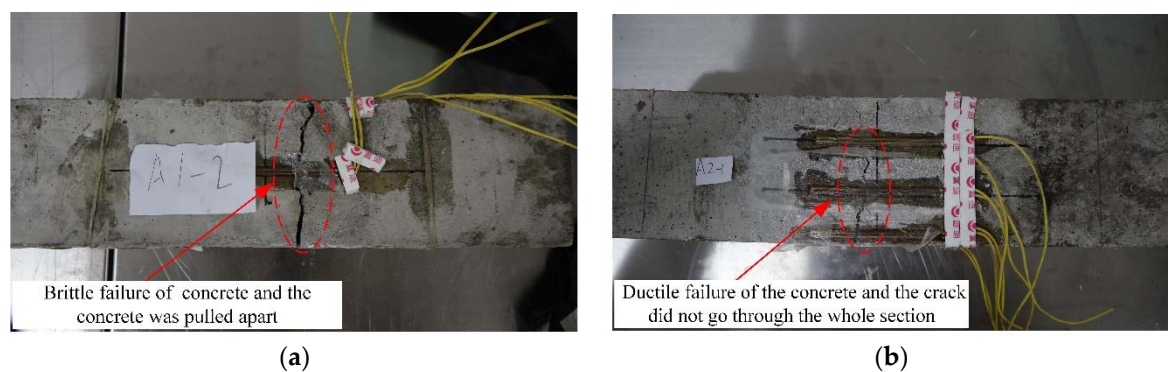


Figure 4. Cont.



Figure 4. The failure modes of specimens. (a) B0.0P0.0; (b) B0.0P6.0; (c) B6.0P0; (d) B2P4.

For the control group specimen B0P0 and the mono-basalt FRC specimen B6P0, the crack rapidly expands to the top of the specimen and runs through the entire section after it appears. Thus, the concrete was pulled apart. It shows that the failure modes of both B0P0 and B6P0 are characterized by brittle failure (see Figure 4a,c), although B6P0 shows a little higher flexural strength. It can be seen that the addition of mono-BF won't improve much of the brittleness of concrete. However, for the mono-polypropylene FRC specimen B0P6 and HBPFR specimen B2P4, after the crack appears, it first rapidly expands to about 2/3 the height of the section. Then, it slowly expands towards the top of the specimen, but it did not run through the entire section during the whole test. The macro PPF in the specimen plays a significant role in bridging; thus, the beam can still show a certain bearing capacity and a long load-bearing time after the crack appears. It shows that the failure modes of both B0P6 and B2P4 change from the sudden brittle failure of plain concrete to ductile failure (see Figure 4b,d). It can be seen that the addition of macro PPF will largely improve the brittleness of concrete.

3.2. Load-Deflection Curve

The load-deflection curves of each group of HBPFR specimens are shown in Figure 5a–g. According to Figure 5a–g, it can be seen that for the control group specimen B0P0 and the mono-basalt FRC specimen B6P0, the load of which immediately decreased to zero after it reached the peak value. B0P0 and B6P0 showed obvious brittleness, and they fractured into two parts in the middle. However, compared with B0P0, the descending stage of B6P0 was relatively slow, indicating the brittleness of concrete is somewhat improved due to the addition of mono-BF.

As for the specimens with macro PPF, although the bearing capacity of these specimens will drop instantly after reaching the peak load, they still maintain a certain residual strength and will not break during the whole test process. It was found that the macro PPF was continuously pulled out and broken during the loading process, which reflected the noticeable bridging effect of the fiber. The descending stage of the load-deflection curves fluctuated to some extent locally due to the pulled out and broken of fibers. Still, the curves were generally gentle, and even the phenomenon of secondary peak appeared in different degrees. Among them, the secondary peak values of B0P6 and B2P4 were particularly apparent (see Figure 5b–e). It can be seen that the addition of macro propylene fiber significantly improves the bending performance of concrete specimens.

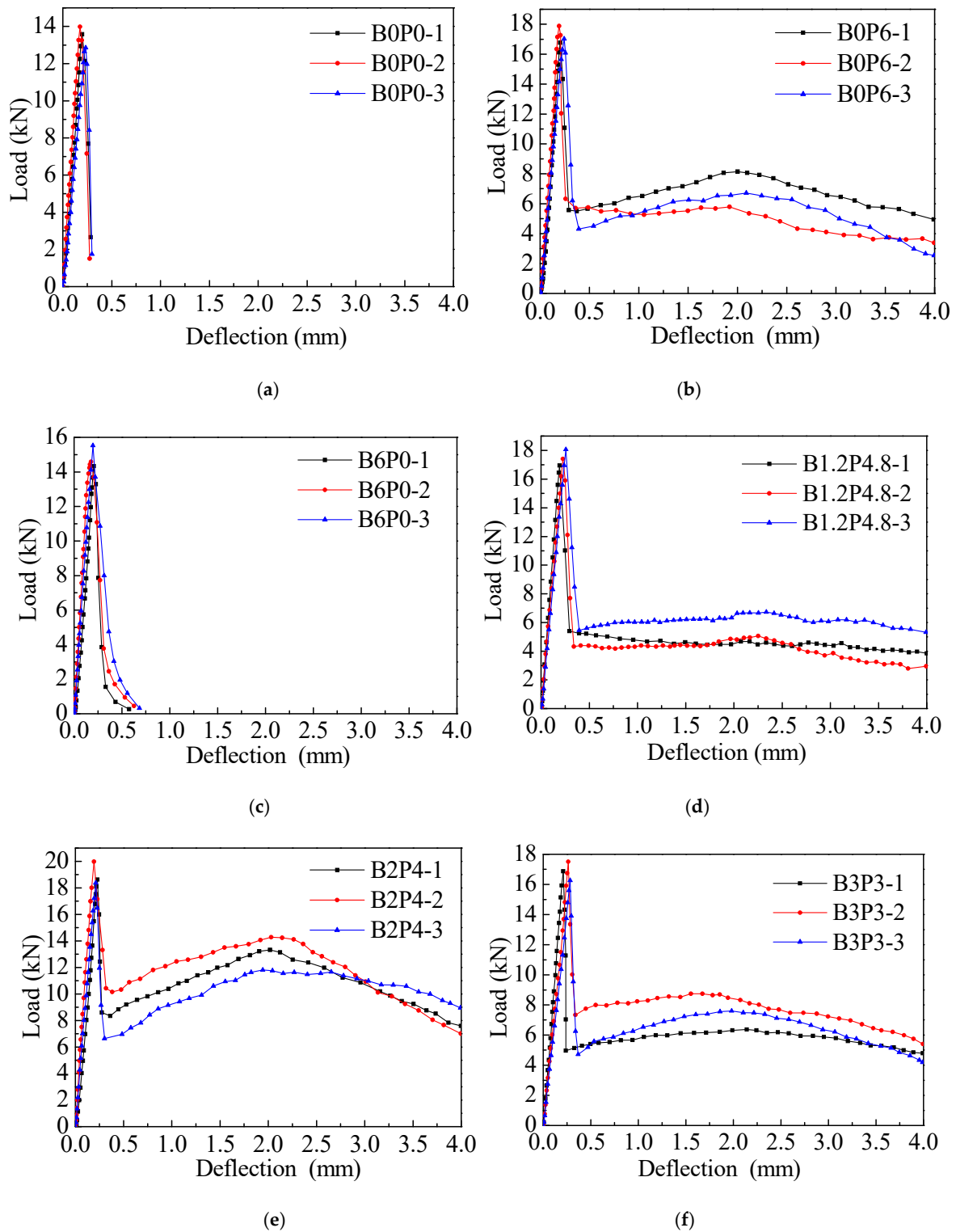


Figure 5. Cont.

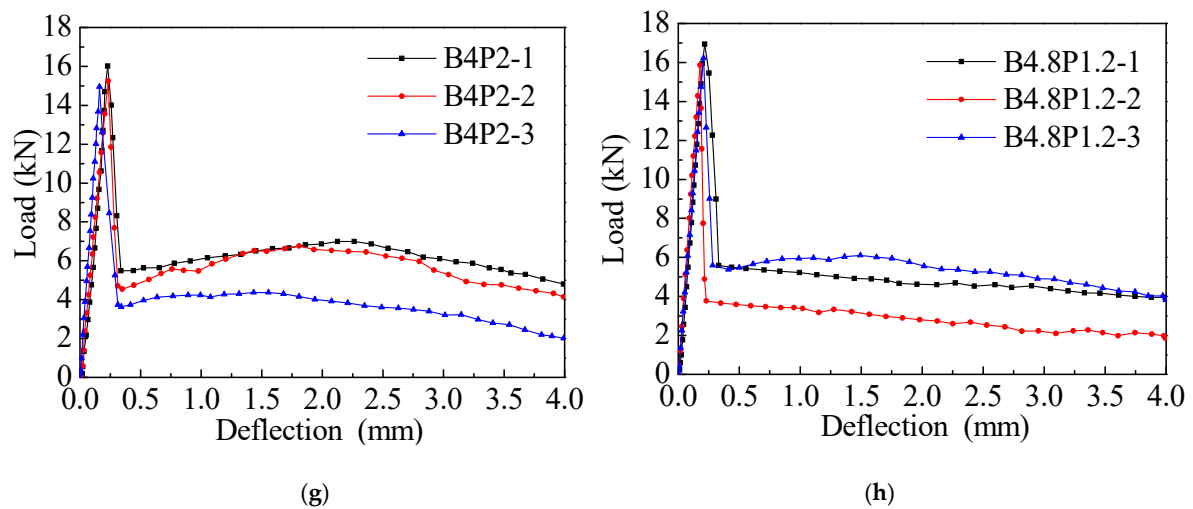


Figure 5. Load-deflection curve of HBPFR specimens. (a) B0.0P0.0; (b) B0.0P6.0; (c) B6.0P0; (d) B1.2P4.8; (e) B2P4; (f) B3.0P3.0; (g) B4.0P2.0; (h) B4.8P1.2.

3.3. Flexural Strength

The peak load of each group specimen is extracted, and then the flexural strength of concrete is calculated by Equation (1):

$$f_b = \frac{P \cdot L}{b \cdot h^2} \quad (1)$$

where f_b is the flexural, MPa; P is peak load, N; L is the span of the specimen, mm; b is the section width of the specimen, mm; H is the height of the specimen section, mm.

The flexural strengths of FRC specimens in this test are shown in Figure 6.

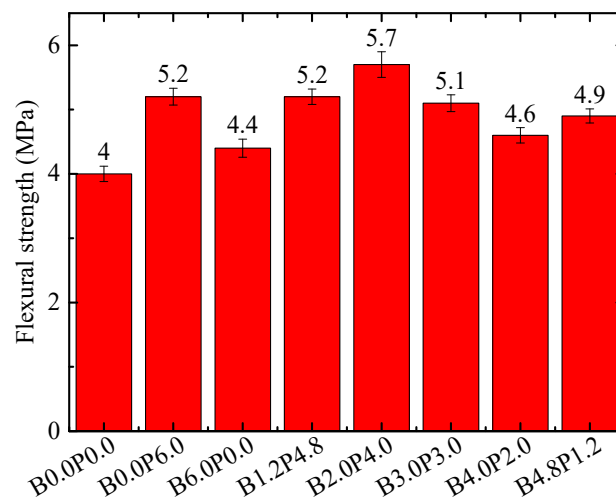


Figure 6. Flexural strength of FRC specimens.

As shown in Figure 6, the flexural strength of the control group specimen B0P0 is 4.0 MPa, while the flexural strength of the mono-basalt FRC specimen B6P0 is 4.4 MPa, increased by 10%. As for the flexural strength of the mono-macro polypropylene FRC specimen B0P6, it increases to 5.2 MPa with a growth rate of 30%. It can be seen that the improvement effect of macro PPF on the flexural strength of concrete specimens is more significant than that of BF. Among the HBPFR specimens, when the mass ratio of BF to macro PPF is 1:2, the flexural strength of the specimen B2P4 reached 5.7 MPa, and the

flexural strength increased the most, reaching 42.5%. This may be due to the good hybrid effect of BF and macro PPF with this hybrid ratio.

3.4. Flexural Toughness

Flexural toughness (T_b) is used to describe the energy absorption capacity of concrete quantitatively. The flexural toughness evaluation method suggested by JSCE-SF4 [8] is adopted in this paper, which does not need to determine the deflection of the initial crack point, and the unstable section of the curve has little influence on it. Flexural toughness is defined as the envelope area of the load-deflection curve under deflection from 0 mm to 1/150 L (2 mm). Because control group specimens and mono-basalt FRC specimens showed brittle failure during the loading process, the flexural toughness of which are calculated by the envelope area of all load-deflection curves according to the literature [55]. Figure 7 shows the flexural toughness of different concrete specimens.

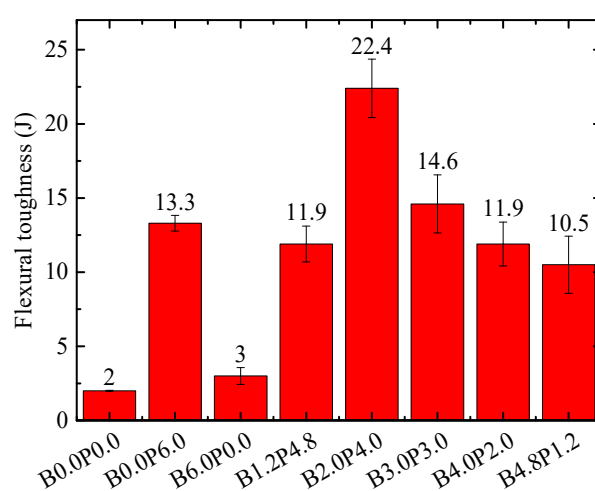


Figure 7. Flexural toughness of FRC specimens.

It can be seen from Figure 7 that the flexural toughness of the control group specimen B0P0 is only 2.0 J, while the flexural toughness of the mono-basalt FRC specimen B6P0 is 3.0 J, increasing by 50%. The flexural strength of mono-macro PPFRC (B0P6) is 13.3 J, which is 5.65 times higher than that of the control group. Compared with BF, the macro PPF has a more significant effect on improving the flexural strength of concrete. Among the HBPFR specimens, the flexural toughness of B4.8P1.2 is the lowest, but it is still 4.25 times higher than that of the control group specimen B0P0. When the mass ratio of BF to PPF is 1:2, the flexural toughness of the specimen B2P4 reached 22.4 J, and it increased by 10.2 times. In conclusion, the flexural toughness of PPF reinforced concrete specimen is better than that of BF reinforced concrete specimen. Because of the fiber mixing effect, the specimens with mixed fiber reinforced concrete can show much better flexural performance than that of the specimens reinforced by mono-macro fiber when the mixing ratio of BF to PPF is 1:2.

Furthermore, the equivalent flexural strength and the percentage of equivalent flexural strength of each group were calculated according to the following Equations (2) and (3), respectively.

$$f_e = \frac{T_b}{\delta_{tb}} \cdot \frac{L}{b \cdot h^2} \quad (2)$$

$$\lambda_e = f_e / f_b \quad (3)$$

where f_e is equivalent flexural strength, MPa; δ_{tb} is mid-span deflection, mm; λ_e is the percentage of equivalent flexural strength. The equivalent flexural strength and Equivalent flexural strength ratio of each group are shown in Figures 8 and 9, respectively.

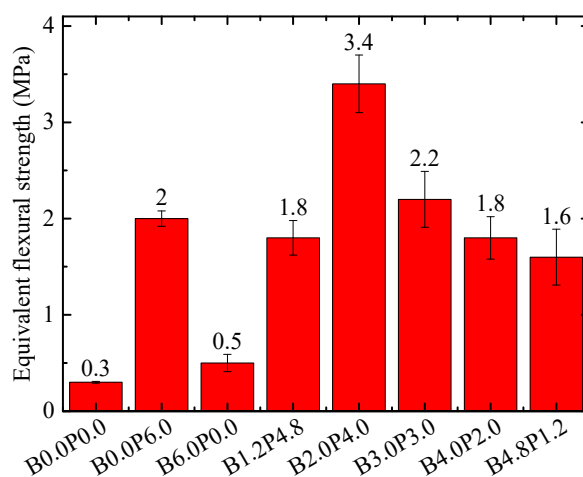


Figure 8. Equivalent flexural strength of FRC specimens.

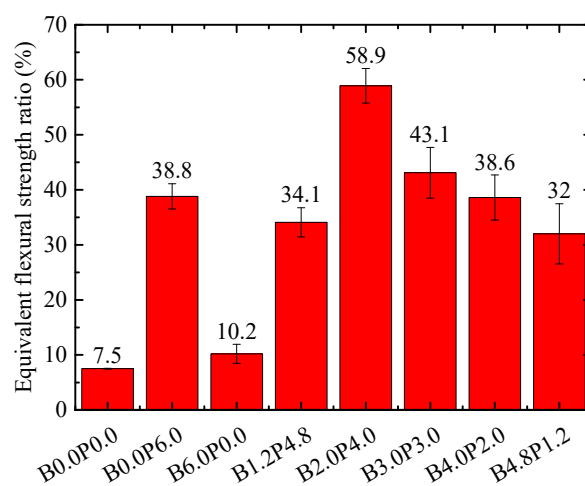


Figure 9. Equivalent flexural strength ratio of FRC specimens.

As shown in Figures 7 and 8, the equivalent flexural strength and flexural toughness of each group of specimens show a consistent variation trend. This is due to that the equivalent flexural strength is just the flexural toughness multiplied by $\frac{1}{\delta_{ib}} \cdot \frac{L}{b \cdot h^2}$, and for the specimen of the same size, the value is constant [55]. As shown in Figure 9, there is a certain difference between the variation trend of equivalent flexural strength and that of equivalent flexural strength ratio. For instance, the equivalent flexural strength of B6P0 is 10.2%, which is only 36% higher than that of the control group B0P0. However, the equivalent flexural strength ratios of specimens containing macro polypropylene were all above 30%, which were at least 3.3 times higher than that of the control group. Among the HBPFR specimens, when the mass ratio of BF to PPF is 1:2, the equivalent flexural strength ratio of the specimen B2P4 is the largest, which is 7.1 times higher than that of the control group.

4. Discussion

4.1. Analysis of the Mechanism of Hybrid Fibers

This study shows that the hybrid of fibers in concrete can effectively improve the brittleness of concrete, and the HBPFR specimens show better flexural ductility than that of plain concrete specimens, which can be attributed to that the fiber can improve various original defects in the concrete matrix and inhibit the development of cracks in loading stage [46]. The role of fiber in improving the bending performance of concrete specimens is played throughout the whole process, from the pouring of concrete and the failure of it.

In the casting stage, during the hardening process of the concrete matrix, the existence of fiber can restrain the micro-cracks caused by plastic shrinkage and temperature deformation, which not only reduces the number of cracks but also reduces the size of cracks. So, it is beneficial to reduce the stress intensity factor at the crack tip. At the loading stage of the specimens, the fiber dissipates the stress concentration at the crack tip, thus limiting the crack propagation. Micro BF and macro PPF play different roles in different stages.

BFs are randomly distributed in the concrete matrix, and these play a favorable role in connecting internal macrocracks. At the same time, due to the extremely high elastic modulus of BF, it can withstand greater tensile stress under smaller strain conditions. Before the appearance of macro-cracks, it requires a large amount of energy to break itself during the expansion process of micro-crack, so that the micro BF can improve the bending performance of concrete. However, due to the low fracture elongation rate of BF, the BF will be immediately broken or pulled out once the macro-crack appears. So the mono addition of BFs cannot effectively improve the brittleness of concrete. As for the macro PPF, it plays a bridging role and shares the load borne by the concrete matrix in the process of crack evolution from micro-crack to macro-crack. Figure 10 is a schematic diagram of the bridging action of macro PPF.

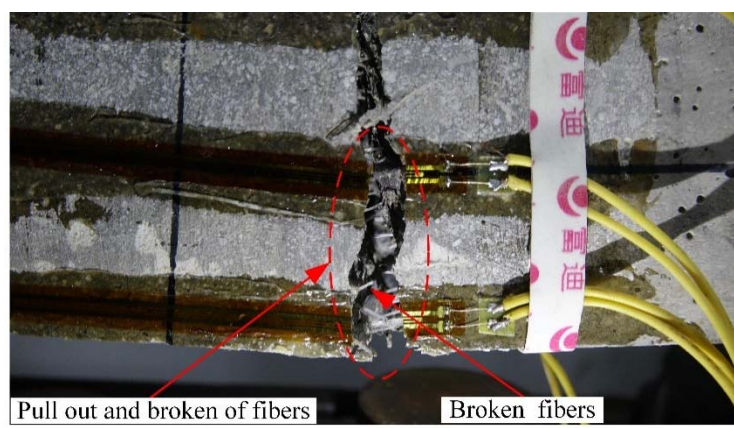


Figure 10. Schematic diagram of the bridging action of macro PPFs.

As shown in Figure 10, in the process of the crack extending upward from the bottom of the specimen, the fibers across the crack will continuously participate in sharing the stress of the concrete matrix. The lower PPFs were continuously pulled out or broken as the crack width increases. At the same time, the upper fiber will successively participate in bearing the load. With the increase of crack width, the load shared by the macro PPFs gradually increases until it is pulled out or broken, which is the reason why the concrete containing the coarse PPFs still has the residual strength for a long time after the peak load. Besides, due to the high elongation capacity of the macro PPF, these are capable to bridge wide cracks without breaking. During the process of crack propagating to the top of the specimen, the number of upper PPFs playing the role of fiber bridging increased, while the lower PPFs can still withstand the tensile force before it is broken. Thus, the total number of fibers playing the role of fiber bridging may increase when the crack propagates. Therefore, the cumulative effect of effective fiber bridging will lead to the second peak value of HBPFR specimens (such as Figure 5b,e–g).

From the above analysis, it can be seen that BF and coarse PPF cannot be substituted for each other in improving the bending performance of concrete. These two fibers play a role in different loading periods of concrete. The bending performance of concrete can be improved by adding two kinds of fibers into concrete collectively in a certain proportion. Due to the positive hybrid effect of fiber, the B2P4 specimen obtained the optimal bending performance.

4.2. Technology and Economic Analysis

Compared with steel fiber, macro PPF has a lower price, less labor cost, strong corrosion resistance and less carbon dioxide emission in the production process [56–58]. Therefore, macro PPF has been used to replace steel fiber in recent years. What is more, as BF is a more environmentally friendly material compared with traditional reinforced concrete materials, it is more environmentally friendly to mix with PPF to produce FRC.

In terms of price, the BF used is 25 China Yuan (CNY)/kg, while the macro PPF is 35 CNY/kg (2019 price). The cost per cubic meter of fiber for each group is shown in Table 5, where the cost-effectiveness is defined as the ratio between the improvement value of the test bending performance of each group compared with the control group and the corresponding fiber cost [59].

Table 5. Price of fibers and cost-effectiveness for per cubic meter FRC.

Specimen	Total Price (CNY)	Flexural Strength (MPa)	Flexural Toughness (J)	Cost-Effectiveness	
				Flexural Strength (kPa/CNY)	Flexural Toughness (10^{-3} J/CNY)
B0.0P0.0	0	4	2	/	/
B0.0P6.0	210	5.2	13.3	5.7	53.8
B6.0P0.0	150	4.4	3	2.7	6.7
B1.2P4.8	198	5.2	11.9	6.1	50.0
B2P4	190	5.7	22.4	8.9	107.4
B3.0P3.0	180	5.1	14.6	6.1	70.0
B4.0P2.0	170	4.6	11.9	3.5	58.2
B4.8P1.2	162	4.9	10.5	5.6	52.5

As shown in Table 5, the total price is lower when the amount of BF is more significant since the price of BF is lower than that of PPF. Although the price of mono-basalt FRC specimen B6P0 is low, it shows the characteristics of brittle failure when subjected to bending force and the increase in flexural strength and toughness is relatively small compared with that of the control group specimen B0P0. Thus, the addition of BF alone cannot effectively improve the bending performance of concrete. Among the HBPFR specimens, the price of B2P4 is not the lowest, but it is only increased by 17.2% compared with that of the HBPFR specimens B4.8P1.2 with the lowest price. However, when compared with the B4.8P1.2 specimen, the flexural strength and flexural toughness of B2P4 increased by 16.3% and 113%, separately. Thus, the selection of B2P4 specimen will significantly improve the energy dissipation capacity of concrete material with a small increase in cost. As for the mono-polypropylene FRC specimen, although it shows high flexural strength and high flexural toughness, it has no advantages compared with the B2P4 group in terms of technology and economy. What is more, B2P4 obtained the highest cost-effectiveness of both flexural strength (8.9 kPa/CNY) and flexural toughness (107.4×10^{-3} J/CNY). Therefore, based on comprehensive technical and economic analysis, it can be seen that the B2P4 group is the test group with the optimal ratio.

5. Conclusions

- (1) The addition of mono-BF proved not to enhance the concrete ductility, while the macro PPF significantly improve the brittleness of concrete and makes the failure modes of PPFRC and HBPFRs change from the sudden brittle failure of plain concrete to ductile failure.
- (2) The addition of hybrid BF and PPF can effectively improve the flexural strength of concrete. Further, the addition of macro PPF proved to increase the post-cracking flexural toughness of concrete. Compared with the control group, when the mass ratio of BF to PPF is 1:2, the flexural toughness and equivalent flexural strength of the

HBPFR specimen were increased by 10.2 times, and the percentage of equivalent flexural strength of it was increased by 7.1 times.

- (3) BF mainly improves the flexural performance of concrete before the occurrence of macro-cracks, while the macro PPF plays the bridging role and improves the flexural performance of concrete in the process of crack evolution from micro-crack to the macro-crack.
- (4) B2P4 specimen significantly improves the energy dissipation capacity of concrete material with just a small increase in cost. From the perspective of both technology and economy, when the mass ratio of BF to PPF is 1:2, the bending performance and economic benefits of FRC reach the optimal level, and this mix ratio is the optimal fiber mixing ratio in this test.

Author Contributions: Conceptualization, Z.D., X.L. and A.d.l.F.; funding acquisition, X.L. and A.d.l.F.; investigation, N.L. and H.P.; methodology, Z.D. and X.L.; resources, N.L.; writing—original draft, Z.D.; writing—review and editing, A.d.l.F. and H.P. All authors have read and agreed to the published version of the manuscript.

Funding: This research project was funded by the Spanish Ministry of Science and Innovation for the financial support received under the scope of the project CREEF (PID2019-108978RB-C32), the National Key Research and Development Program of China (Grant No. 2018YFC1504802), Natural Science Foundation Project of Chongqing (Grant No. cstc2018jscx-mszdX0071) and National Natural Science Foundation of China (Grant No. 41772319).

Data Availability Statement: All data are in the paper.

Conflicts of Interest: The authors declare that they have no conflict of interest.

References

1. Guerini, V.; Conforti, A.; Plizzari, G.; Kawashima, S. Influence of Steel and Macro-Synthetic Fibers on Concrete Properties. *Fibers* **2018**, *6*, 47. [\[CrossRef\]](#)
2. Das, C.S.; Dey, T.; Dandapat, R.; Mukharjee, B.B.; Kumar, J. Performance evaluation of polypropylene fibre reinforced recycled aggregate concrete. *Constr. Build. Mater.* **2018**, *189*, 649–659. [\[CrossRef\]](#)
3. Okeola, A.A.; Abuodha, S.O.; Mwero, J. Experimental Investigation of the Physical and Mechanical Properties of Sisal Fiber-Reinforced Concrete. *Fibers* **2018**, *6*, 53. [\[CrossRef\]](#)
4. Kytinou, V.K.; Chalioris, C.E.; Karayannis, C.G. Analysis of Residual Flexural Stiffness of Steel Fiber-Reinforced Concrete Beams with Steel Reinforcement. *Materials* **2020**, *13*, 2698. [\[CrossRef\]](#) [\[PubMed\]](#)
5. Chalioris, C.; Panagiotopoulos, T.A. Flexural analysis of steel fibre-reinforced concrete members. *Comput. Concr.* **2018**, *22*, 11–25. [\[CrossRef\]](#)
6. Choi, S.-W.; Choi, J.; Lee, S.-C. Probabilistic Analysis for Strain-Hardening Behavior of High-Performance Fiber-Reinforced Concrete. *Materials* **2019**, *12*, 2399. [\[CrossRef\]](#)
7. Jain, K.; Singh, B. Deformed steel fibres as minimum shear reinforcement—An investigation. *Structures* **2016**, *7*, 126–137. [\[CrossRef\]](#)
8. JSCE-SF4. *Standard for Flexural Strength and Flexural Toughness, Method of Tests for Steel Fiber Reinforced Concrete*; Concrete Library of JSCE, Japan Concrete Institute (JCI): Tokyo, Japan, 1984; pp. 58–66.
9. ASTM C1018-97. *Standard Test Method for Flexural Toughness and First-Crack Strength of Fiber-Reinforced Concrete (Using Beam with Third-Point Loading)*; ASTM International: West Conshohocken, PA, USA, 1997. [\[CrossRef\]](#)
10. CECS 13:2009. *Standard Test Methods for Fiber Reinforced Concrete*; Chinese Association Standards of Engineering Construction Standardization: Beijing, China, 2009.
11. Buratti, N.; Mazzotti, C.; Savoia, M. Post-cracking behaviour of steel and macro-synthetic fibre-reinforced concretes. *Constr. Build. Mater.* **2011**, *25*, 2713–2722. [\[CrossRef\]](#)
12. Nicolaides, D.; Markou, G. Modelling the flexural behaviour of fibre reinforced concrete beams with FEM. *Eng. Struct.* **2015**, *99*, 653–665. [\[CrossRef\]](#)
13. Pujadas, P.; Blanco, A.; Cavalaro, S.H.P.; De La Fuente, A.; Aguado, A. Flexural Post-cracking Creep Behaviour of Macro-synthetic and Steel Fiber Reinforced Concrete. In *Creep Behaviour in Cracked Sections of Fibre Reinforced Concrete*; Serna, P., Llano-Tore, A., Cavalaro, S.H.P., Eds.; Springer: Berlin/Heidelberg, Germany, 2017; pp. 77–87.
14. Enfedaque, A.; Alberti, M.G.; Galvez, J.; Beltrán, M. Constitutive relationship of polyolefin fibre-reinforced concrete: Experimental and numerical approaches to tensile and flexural behaviour. *Fatigue Fract. Eng. Mater. Struct.* **2018**, *41*, 358–373. [\[CrossRef\]](#)
15. Li, B.; Chi, Y.; Xu, L.; Shi, Y.; Li, C. Experimental investigation on the flexural behavior of steel-polypropylene hybrid fiber reinforced concrete. *Constr. Build. Mater.* **2018**, *191*, 80–94. [\[CrossRef\]](#)

16. Mínguez, J.; González, D.C.; Vicente, M.A. Fiber geometrical parameters of fiber-reinforced high strength concrete and their influence on the residual post-peak flexural tensile strength. *Constr. Build. Mater.* **2018**, *168*, 906–922. [\[CrossRef\]](#)
17. Liu, F.; Ding, W.; Qiao, Y. Experimental investigation on the flexural behavior of hybrid steel-PVA fiber reinforced concrete containing fly ash and slag powder. *Constr. Build. Mater.* **2019**, *228*, 116706. [\[CrossRef\]](#)
18. Carrillo, J.; Torres, D.; Guerrero, H. Correlation between results obtained from four-point bending tests (4PBT) and double punch tests (DPT) in concrete reinforced with hooked-end steel fibers. *Eng. Struct.* **2021**, *239*, 112353. [\[CrossRef\]](#)
19. Ferdosian, I.; Camões, A. Mechanical performance and post-cracking behavior of self-compacting steel-fiber reinforced eco-efficient ultra-high performance concrete. *Cem. Concr. Compos.* **2021**, *121*, 104050. [\[CrossRef\]](#)
20. Guo, H.; Jiang, L.; Tao, J.; Chen, Y.; Zheng, Z.; Jia, B. Influence of a hybrid combination of steel and polypropylene fibers on concrete toughness. *Constr. Build. Mater.* **2021**, *275*, 122132. [\[CrossRef\]](#)
21. Meng, G.; Wu, B.; Xu, S.; Huang, J. Modelling and experimental validation of flexural tensile properties of steel fiber reinforced concrete. *Constr. Build. Mater.* **2021**, *273*, 121974. [\[CrossRef\]](#)
22. Abadel, A.; Abbas, H.; Almusallam, T.; Al-Salloum, Y.; Siddiqui, N. Mechanical properties of hybrid fibre-reinforced concrete—analytical modelling and experimental behaviour. *Mag. Concr. Res.* **2016**, *68*, 1–21. [\[CrossRef\]](#)
23. Yang, X.; Liang, N.; Liu, X.; Zhong, Z. A study of test and statistical damage constitutive model of multi-size polypropylene fiber concrete under impact load. *Int. J. Damage Mech.* **2018**, *28*, 973–989. [\[CrossRef\]](#)
24. Koniki, S.; Prasad, D.R. Influence of hybrid fibres on strength and stress-strain behaviour of concrete under uniaxial stresses. *Constr. Build. Mater.* **2019**, *207*, 238–248. [\[CrossRef\]](#)
25. Bošnjak, J.; Sharma, A.; Grauf, K. Mechanical Properties of Concrete with Steel and Polypropylene Fibres at Elevated Temperatures. *Fibers* **2019**, *7*, 9. [\[CrossRef\]](#)
26. Afroughsabet, V.; Ozbakkaloglu, T. Mechanical and durability properties of high-strength concrete containing steel and polypropylene fibers. *Constr. Build. Mater.* **2015**, *94*, 73–82. [\[CrossRef\]](#)
27. Nataraja, M.; Dhang, N.; Gupta, A. Stress–strain curves for steel-fiber reinforced concrete under compression. *Cem. Concr. Compos.* **1999**, *21*, 383–390. [\[CrossRef\]](#)
28. Betterman, L.; Ouyang, C.; Shah, S. Fiber-matrix interaction in microfiber-reinforced mortar. *Adv. Cem. Based Mater.* **1995**, *2*, 53–61. [\[CrossRef\]](#)
29. Banthia, N.; Majdzadeh, F.; Wu, J.; Bindiganavile, V. Fiber synergy in Hybrid Fiber Reinforced Concrete (HyFRC) in flexure and direct shear. *Cem. Concr. Compos.* **2014**, *48*, 91–97. [\[CrossRef\]](#)
30. Kasagani, H.; Rao, C. Effect of graded fibers on stress strain behaviour of Glass Fiber Reinforced Concrete in tension. *Constr. Build. Mater.* **2018**, *183*, 592–604. [\[CrossRef\]](#)
31. Wang, D.; Ju, Y.; Shen, H.; Xu, L. Mechanical properties of high performance concrete reinforced with basalt fiber and polypropylene fiber. *Constr. Build. Mater.* **2019**, *197*, 464–473. [\[CrossRef\]](#)
32. Soe, K.T.; Zhang, Y.; Zhang, L. Material properties of a new hybrid fibre-reinforced engineered cementitious composite. *Constr. Build. Mater.* **2013**, *43*, 399–407. [\[CrossRef\]](#)
33. Zhang, C.; Han, S.; Hua, Y. Flexural performance of reinforced self-consolidating concrete beams containing hybrid fibers. *Constr. Build. Mater.* **2018**, *174*, 11–23. [\[CrossRef\]](#)
34. Caetano, H.; Rodrigues, J.P.C.; Pimienta, P. Flexural strength at high temperatures of a high strength steel and polypropylene fibre concrete. *Constr. Build. Mater.* **2019**, *227*, 116721. [\[CrossRef\]](#)
35. Bhogone, M.V.; Subramaniam, K.V.L. Early-age tensile constitutive relationships for steel and polypropylene fiber reinforced concrete. *Eng. Fract. Mech.* **2021**, *244*, 107556. [\[CrossRef\]](#)
36. Jiang, C.; Fan, K.; Wu, F.; Chen, D. Experimental study on the mechanical properties and microstructure of chopped basalt fibre reinforced concrete. *Mater. Des.* **2014**, *58*, 187–193. [\[CrossRef\]](#)
37. Branston, J.; Das, S.; Kenno, S.Y.; Taylor, C. Mechanical behaviour of basalt fibre reinforced concrete. *Constr. Build. Mater.* **2016**, *124*, 878–886. [\[CrossRef\]](#)
38. Borhan, T.M. Properties of glass concrete reinforced with short basalt fibre. *Mater. Des.* **2012**, *42*, 265–271. [\[CrossRef\]](#)
39. Sim, J.; Park, C.; Moon, D.Y. Characteristics of basalt fiber as a strengthening material for concrete structures. *Compos. Part. B Eng.* **2005**, *36*, 504–512. [\[CrossRef\]](#)
40. Kizilkanat, A.B.; Kabay, N.; Akyüncü, V.; Chowdhury, S.; Akça, A.H. Mechanical properties and fracture behavior of basalt and glass fiber reinforced concrete: An experimental study. *Constr. Build. Mater.* **2015**, *100*, 218–224. [\[CrossRef\]](#)
41. Fu, Q.; Niu, D.; Li, D.; Wang, Y.; Zhang, J.; Huang, D. Impact characterization and modelling of basalt-polypropylene fibre-reinforced concrete containing mineral admixtures. *Cem. Concr. Compos.* **2018**, *93*, 246–259. [\[CrossRef\]](#)
42. Zhang, H.; Wang, L.; Bai, L.; Addae, M.; Neupane, A. Research on the impact response and model of hybrid basalt-macro synthetic polypropylene fiber reinforced concrete. *Constr. Build. Mater.* **2019**, *204*, 303–316. [\[CrossRef\]](#)
43. Fu, Q.; Niu, D.; Zhang, J.; Huang, D.; Hong, M. Impact response of concrete reinforced with hybrid basalt-polypropylene fibers. *Powder Technol.* **2018**, *326*, 411–424. [\[CrossRef\]](#)
44. Smarzewski, P. Flexural Toughness of High-Performance Concrete with Basalt and Polypropylene Short Fibres. *Adv. Civ. Eng.* **2018**, *2018*, 1–8. [\[CrossRef\]](#)
45. Smarzewski, P. Influence of basalt-polypropylene fibres on fracture properties of high performance concrete. *Compos. Struct.* **2019**, *209*, 23–33. [\[CrossRef\]](#)

46. Liang, N.; Zhong, Y.; Liu, X. Experimental study of flexural toughness for multi-scale polypropylene fiber reinforced concrete. *J. Cent. South Univ.* **2017**, *48*, 2783–2789. (In Chinese)
47. Deng, Z.; Liu, X.; Yang, X.; Liang, N.; Yan, R.; Chen, P.; Miao, Q.; Xu, Y. A study of tensile and compressive properties of hybrid basalt-polypropylene fiber-reinforced concrete under uniaxial loads. *Struct. Concr.* **2021**, *22*, 396–409. [[CrossRef](#)]
48. Pujadas, P.; Blanco, A.; Cavalaro, S.; Aguado, A. Plastic fibres as the only reinforcement for flat suspended slabs: Experimental investigation and numerical simulation. *Constr. Build. Mater.* **2014**, *57*, 92–104. [[CrossRef](#)]
49. Pujadas, P.; Blanco, A.; Cavalaro, S.H.P.; De La Fuente, A.; Aguado, A. The need to consider flexural post-cracking creep behavior of macro-synthetic fiber reinforced concrete. *Constr. Build. Mater.* **2017**, *149*, 790–800. [[CrossRef](#)]
50. De la Fuente, A.; Escariz, R.C.; Figueiredo, A.; Aguado, A. Design of macro-synthetic fibre reinforced concrete pipes. *Constr. Build. Mater.* **2013**, *43*, 523–532. [[CrossRef](#)]
51. De la Fuente, A.; Escariz, R.C.; Figueiredo, A.; Molins, C.; Aguado, A. A new design method for steel fibre reinforced concrete pipes. *Constr. Build. Mater.* **2012**, *30*, 547–555. [[CrossRef](#)]
52. De La Fuente, A.; De Figueiredo, A.D.; Aguado, A.; Molins, C.; Neto, P.J.C.; Figueiredo, A. Experimentación y simulación numérica de tubos de hormigón con fibras. *Mater. Constr.* **2010**, *61*, 275–288. [[CrossRef](#)]
53. Deng, Z.; Liu, X.; Chen, P.; de la Fuente, A.; Zhou, X.; Liang, N.; Han, Y.; Du, L. Basalt-polypropylene fiber reinforced concrete for durable and sustainable pipe production. Part 1: Experimental program. *Struct. Concr.* **2021**. [[CrossRef](#)]
54. Deng, Z.; Liu, X.; Chen, P.; de la Fuente, A.; Zhao, Y.; Liang, N.; Zhou, X.; Du, L.; Han, Y. Basalt-polypropylene fiber reinforced concrete for durable and sustainable pipe production. Part 2: Numerical and parametric analysis. *Struct. Concr.* **2021**. [[CrossRef](#)]
55. Soutsos, M.; Le, T.; Lampropoulos, A. Flexural performance of fibre reinforced concrete made with steel and synthetic fibres. *Constr. Build. Mater.* **2012**, *36*, 704–710. [[CrossRef](#)]
56. Shen, L.; Worrell, E.; Patel, M.K. Open-loop recycling: A LCA case study of PET bottle-to-fibre recycling. *Resour. Conserv. Recycl.* **2010**, *55*, 34–52. [[CrossRef](#)]
57. Strezov, L.; Herbertson, J. *A Life Cycle Perspective on Steel Building Materials*; Principals of the Crucible Group Pty Ltd.: Newcastle, Australian, 2006.
58. Yin, S.; Tuladhar, R.; Shi, F.; Combe, M.; Collister, T.; Sivakugan, N. Use of macro plastic fibres in concrete: A review. *Constr. Build. Mater.* **2015**, *93*, 180–188. [[CrossRef](#)]
59. Liu, H.; Liu, Y.; Zhang, X.; Wang, S. Cost performance analysis of fiber-constrained concrete prisms. *China Concr. Cem. Prod.* **2009**, *36*, 46–47. (In Chinese) [[CrossRef](#)]